BY PAUL W. MAY, JAMES D. DOYLE,
JULIE D. PULLEN, AND LAURA T. DAVID

# Two-Way Coupled Atmosphere-Ocean Modeling of the PhilEx Intensive Observational Periods

ABSTRACT. High-resolution coupled atmosphere-ocean simulations of the Philippines show the regional and local nature of atmospheric patterns and ocean response during Intensive Observational Period cruises in January–February 2008 (IOP-08) and February–March 2009 (IOP-09) for the Philippine Straits Dynamics Experiment. Winds were stronger and more variable during IOP-08 because the time period covered was near the peak of the northeast monsoon season. Distinct wind jets between islands and wakes behind islands are common northeast monsoon features that are controlled by winds interacting with island topography. The modeled upper-ocean flow associated with Philippine straits during IOP-08 exhibits large (> 1 m $s^{-1}$) westward mean flow through Suriago Strait and highly variable flow through Mindoro Strait. The model shows prominent eddies in the Bohol Sea and Cuyo East Pass that were also observed during the field experiment. A high-resolution nested simulation of the Verde Island Passage finds local wind-driven upwelling that is confirmed by shipboard sea surface temperature measurements and satellite observations of chlorophyll concentration.

## INTRODUCTION

The Philippine Archipelago is an intricate array of islands, straits, and semi-enclosed seas whose broad atmospheric circulation is governed by the rhythm of the East Asian monsoon and steady Pacific trade winds. Philippine oceanic circulation is dominated by the position of the island chain between the South China Sea to the west and the western Pacific Ocean to the east, with its nearby North Equatorial, Kuroshio, and Mindanao currents. Observational and numerical studies of these global-scale phenomena abound (Qu et al., 2009), but within the island archipelago, there are finer scales at play in both the atmosphere and ocean that have not received as much attention. These smaller-scale winds and currents are primarily controlled by topography and geometry, and they act to complicate and obscure an emerging understanding of the interisland circulation. Exploring the 10–100 km circulation patterns of the Philippines, particularly of the surface winds and upper-ocean currents, requires many observations and the interpretive assistance of high-resolution numerical modeling.

The Naval Research Laboratory (NRL) contributed to the Philippine Straits Dynamics Experiment (PhilEx) Intensive Observational Period research cruises in 2008 and 2009 (IOP-08 and IOP-09) by supplying the shipboard team with real-time atmospheric and oceanic forecasting, and with additional retrospective two-way coupled numerical hindcasts. The forecasts provided information to scientists at sea both for general operations and as guidance for developing underway sampling strategies. The more carefully controlled, a posteriori simulations offer important insights into complex regional

kinematics and dynamics. Although there are other numerical studies of the region (e.g., Metzger and Hurlburt, 1996; Han et al., 2009), the NRL coupled atmosphere-ocean model is a unique tool for simultaneous high-resolution studies of both the meteorology and oceanography of a region.

## COUPLED AIR-SEA MODEL

NRL numerical simulations for the Philippines used the Coupled Ocean/Atmosphere Mesoscale Prediction System (COAMPS), which consists of an atmospheric model coupled with the Navy Coastal Ocean Model (NCOM). The atmospheric model is nonhydrostatic with a terrain-following vertical coordinate (Hodur, 1997), while the ocean model features hydrostatic dynamics, generalized curvilinear horizontal coordinates, a bathymetry-following vertical coordinate, and a free surface (Barron et al., 2006). Air-to-ocean two-way coupling is accomplished through the community-based Earth System Modeling Framework (ESMF; Earth System Modeling, 2010), which allows each model to use flexible, generalized grids and a configurable air-sea coupling interval, typically every 10 to 15 minutes. Atmospheric physical parameterizations for surface fluxes use bulk aerodynamic formulae based on the TOGA-COARE (Tropical Ocean Global Atmosphere-Coupled Ocean Atmosphere Response Experiment) algorithms (Fairall et al., 1996), a level 2.5 Mellor-Yamada boundary layer representation, short- and long-wave radiation parameterization, and moist processes, including explicit microphysical equations for rain, snow, cloud water, cloud ice, and graupel (snow pellets). In the two-way coupling scheme, the atmospheric model passes parameterized surface momentum, heat, and moisture fluxes through ESMF to the ocean model. The ocean, which also uses a Mellor-Yamada level 2.5 turbulent boundary layer mixing scheme, completes the two-way coupling by returning the sea surface temperature through ESMF to act as a lower boundary condition to the atmosphere. The coupled model supports grid nesting, which permits progressively higher resolution with each grid refinement—typically implemented at a 3:1 ratio. Further details of the parameterizations, nesting, and coupling in COAMPS may be found in Chen et al. (2010).

Regional forecast models require external information in the form of initial conditions, lateral boundary conditions, and timely observations. The atmospheric data assimilation of quality-controlled upper-air sounding, surface, commercial aircraft, and satellite data is achieved with the use of a Multivariate Optimum Interpolation (MVOI) scheme. Ocean observations, which include floats, drifters, moorings, satellite sea surface temperatures (SST), conductivity-temperature-depth/expendable bathythermograph (CTD/XBT) profiles, and satellite altimetry, are assimilated by the MVOI-based NRL Coupled Ocean Data Assimilation System (Cummings, 2005). The initial state and lateral boundary conditions for the outermost atmospheric and oceanic nests are from the 1° Navy Operational Global Analysis and Prediction System (NOGAPS) and the operational 1/8° Global NCOM (gNCOM) forecast fields, respectively.

During IOP-08 and IOP-09, daily oceanic and atmospheric COAMPS forecasts were supplied to researchers on the cruises in real time (see Pullen et al., 2011, for details of how the model guidance was used in ship-track planning). Additional simulations, using two-way coupled COAMPS with higher ocean resolutions were run later for the time period that encompassed the IOP-08. From these simulations, a 60-day period covering January through February 2008 and a 40-day period covering February through March 2009 were selected for comparison here. For the 2008 time period, nested atmospheric grid meshes of 27, 9, and 3 km ran above nested ocean grids of 3 and 1 km. There were 40 vertical levels in both the atmosphere and ocean models. After initializing with NOGAPS and gNCOM fields on January 1, 2008, the coupled model was run for 60 days with atmospheric data assimilation cycles every 12 hours. For 2009, nested atmospheric grids of 27 and 9 km were used with a 9-km ocean grid. In the 2009 model, horizontal spatial domains differed slightly from those in 2008, reflecting a ship course that was further south. Also, because of the coarser resolution (9 km) of the ocean model run during the 2009 field experiment, it is not considered in the comparisons. In all the cases presented here, NCOM ran without tidal boundary forcing.

## ATMOSPHERIC FORCING DURING IOP-08 AND IOP-09

Surface wind is an important forcing mechanism for the upper ocean on both global and local scales, and is particularly evident in circulation patterns in and around the Philippine Archipelago. In nearby and surrounding waters,

large-scale stresses from the Pacific trade winds are responsible for the North Equatorial Current and the resulting sea level differences between the western Pacific and the South China Sea. Seasonal monsoon winds are also known to modulate circulation in the adjacent South China Sea (Metzger and Hurlburt, 1996; Qu, 2000). But, local-scale winds also drive important interisland circulations. These local wind characteristics during PhilEx are described by considering the mean and variability of the atmospheric model's 10-m wind. The variability of vector quantities (winds and currents) is concisely summarized by using the eigenvalues and eigenvectors of the vector component's covariance matrix (Emery and Thompson, 1998), which define two principal axes of variability. In this scheme, the axis in the direction of greatest variance, the major principal axis, has a magnitude equal to the standard deviation of the wind or current in that direction. The minor axis is the magnitude and direction of variability that is orthogonal or uncorrelated with the major axis variability.

Mean 10-m winds from the 9-km COAMPS forecasts for January through February 2008 (Figure 1a) clearly show the influence of the northeasterly (winter) monsoon, which is normally strongest at this time of year (Chang, 2004). The mean winds range from 10–12 m $s^{-1}$ in Luzon Strait (20°N, 121°E) to 5–6 m $s^{-1}$ in the southern Sulu Sea (7°N, 120°E). A series of wind-speed maxima and minima are noticeable features on the leeward or downwind side of the Philippine Archipelago (see Figure 1a in Gordon et al., 2011, for locations of major islands and passages). The most prominent wind jets occur (from north to south) at Verde Island Passage (13°30'N, 120°50'E), which separates Luzon and Mindoro islands, and Tablas Strait (12°20'N, 121°40'E), which separates Mindoro and Panay. In Tablas Strait, mean winds exceed 12 m $s^{-1}$ and the jet extends nearly 200 km to the southwest. There are prominent wind maxima or tip jets (Doyle and Shapiro, 1999) at the northern and southern flanks of Mindoro Island. Wind jets are also present in the Panay Gulf/Guimaras Strait (10°20'N, 122°20'E) and Dipolog Strait (8°50'N, 123°10'E), which lies between the islands of Mindanao and Negros. Minima in the mean wind velocities occur on the downwind side of each of the islands: Luzon, Mindoro, Panay, Negros, and Mindanao. These wind jets and associated leeside wakes are caused by the airflow over the mountainous terrain of the Philippine Archipelago. Along this mountainous island chain, several peaks in the Cordillera Central on Luzon exceed 2700 m in elevation, and the highest point in the Philippines, Mount Apo on Mindanao, is more than 2900 m above sea level. The enhanced wind flow in the straits is driven by along-gap pressure gradients that are a consequence of the partial blocking of cross-island monsoon flow by the mountains (e.g., Gabersek and Durran, 2004).

Downstream wakes form from air descent, acceleration, wave breaking, and potential vorticity generation that occur over the islands (Smith et al., 1997). Wakes can be long and straight when the mountain-generated potential vorticity and Coriolis force are weak (e.g., at low latitudes; Smith et al., 1997; Burk et al., 2003). In other situations, with stronger forcing, vortex shedding can ensue (Smolarkiewicz and Rotunno, 1989). Island wakes and wind jets in ocean straits are not uncommon and have been observed in the Hawaiian Islands (Smolarkiewicz et al., 1988; Yoshida et al., 2010), Caribbean (Smith et al., 1997); Tsushima Straits (Shimada and Kawamura, 2008), Aleutians, Sandwich Islands, Madagascar, and numerous other island regions.

It is remarkable that wind variability (Figure 1b) is largest in the wake regions, where unsteady conditions may exist. By contrast, wind variability has relative minima in the wind jet regions where the flow is less influenced by topography and hence less turbulent. In the two most prominent wake regions, those downwind from Luzon and Mindoro islands, the largest variability is nearest the western coast, and the major axis of variability is oriented in a distinctly onshore direction, which likely is associated with strong but intermittent downslope winds that penetrate to the ocean surface and interrupt the wake signature. Another obvious area of large variability is the region to the northwest of Luzon where the monsoon winds are channeled into the South China Sea through Luzon Strait. In this region, the largest wind

**Paul W. May** *(paul.may.ctr@nrlmry.navy.mil) is Research Scientist, Computer Science Corporation, Monterey, CA, USA.* **James D. Doyle** *is Head, Mesoscale Modeling Section, Marine Meteorology Division, Naval Research Laboratory, Monterey, CA, USA.* **Julie D. Pullen** *is Director, Maritime Security Laboratory, Stevens Institute of Technology, Hoboken, NJ, USA.* **Laura T. David** *is Professor, Marine Science Institute, University of the Philippines Diliman, Quezon City, Philippines.*

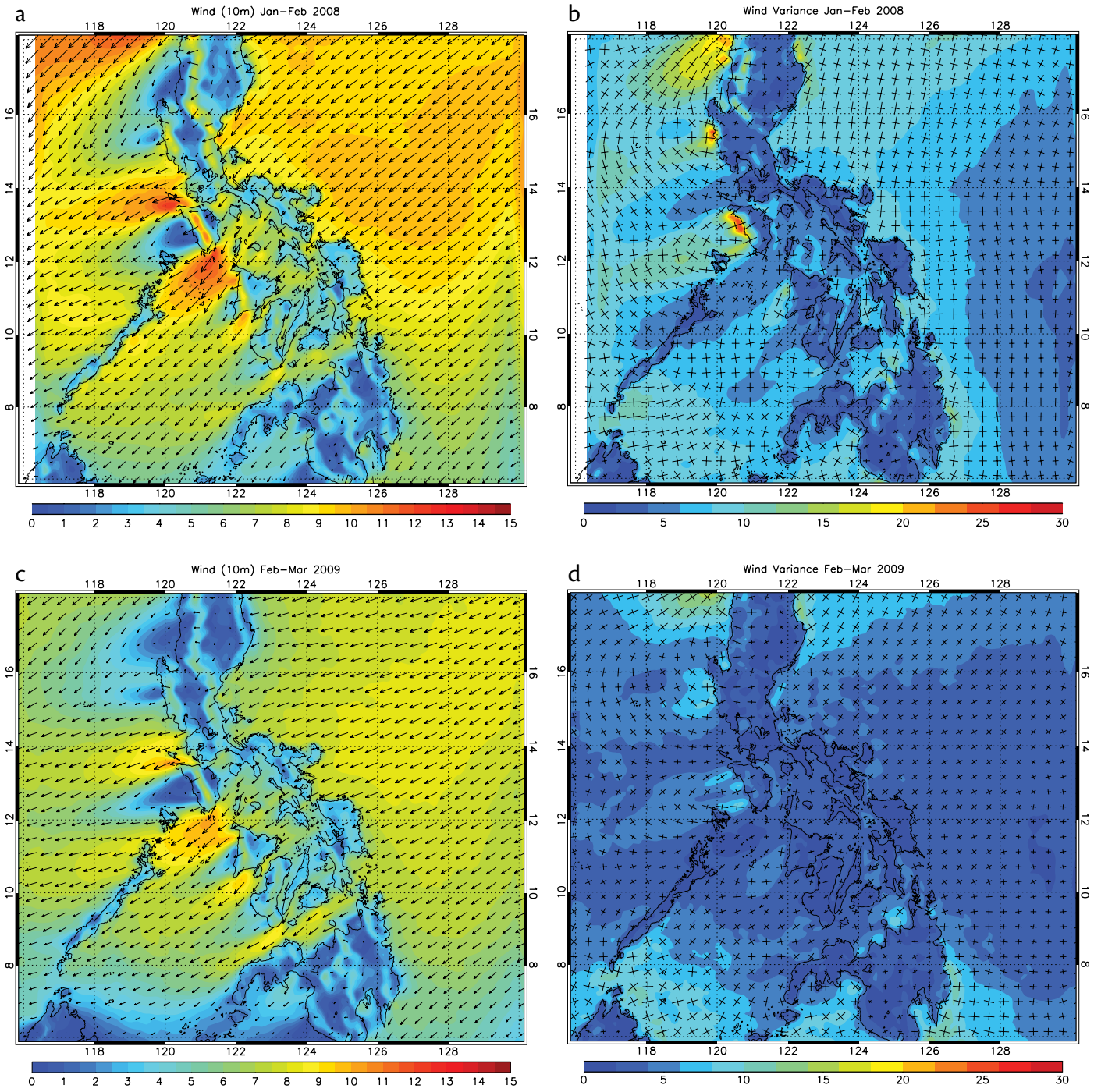


Figure 1. The Coupled Ocean/Atmosphere Mesoscale Prediction System (COAMPS) 10-m mean wind (left panels) and mean variability (right panels) from the 9-km computational grids for the two Intensive Observational Periods (IOPs). Every fifth wind vector and variability cross is plotted. (a) Wind vectors with color-shaded wind speed (m $s^{-1}$) for January to February 2008. (b) Variability vectors with color-shaded variability magnitude ($m^2$ $s^{-2}$) for 2008. (c) Wind vectors plotted over color-shaded wind speed (m $s^{-1}$) for February to March 2009. (d) Variability vectors plotted over color-shaded variability magnitude ($m^2$ $s^{-2}$) for 2009.

variability is associated with strong mean winds, and the orientation of the variability is parallel to the wind. Further south along Luzon, the mean wind direction is relatively unchanged, but the preferred wind variability orientation trends in the alongshore direction where it is, in some cases, at right angles to the mean wind direction.

The mean 10-m winds and wind variability from the COAMPS forecasts that cover the PhilEx IOP-09 period are

averaged over a 40-day period from the middle of February through the end of March 2009 (Figure 1c). During this time, the winds are significantly weaker than those of 2008, indicating a drop in the intensity of the seasonal monsoon. Besides being weaker, the wind direction has more of an easterly component. Wind jets and wakes are still apparent to the west of the Philippines, with the strongest winds again through Verde Island Passage and Tablas Strait, and the weakest winds behind Mindoro and the Cordillera Central in the wake regions. Wind jets over Panay Gulf and through Dipolog Strait are stronger relative to 2008. Again, well-defined wind maxima along the lee slopes of the mountain ridges are clearly evident, which is consistent with the presence of mountain-wave-induced wakes. Wind variability during IOP-09 (Figure 1d) is also uniformly lower than that in 2008, but still shows the lowest variability in island passage jets and highest variability in mountain wakes. Variability in the lee of the mountains has the same distinct onshore-offshore orientation and, as in 2008, the variability in orientation near Luzon Straits shifts directions, possibly an adjustment of the northeast monsoon to the Luzon island wake.

Synthetic aperture radar (SAR) surface wind speeds (Figure 2a), derived from a European Space Agency Envisat Advanced SAR (ASAR) image on

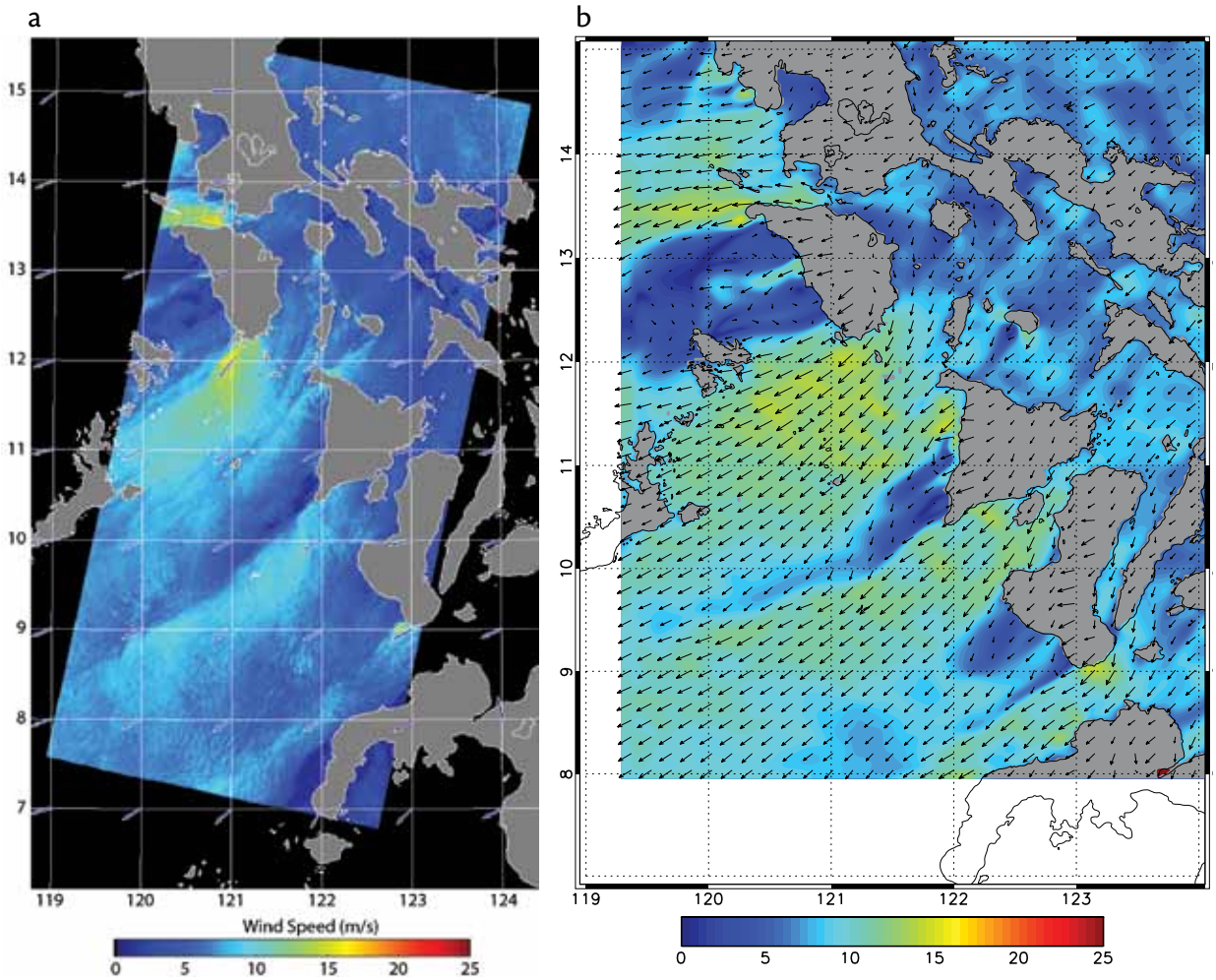


Figure 2. (a) Surface wind speeds derived from an Envisat Advanced Synthetic Aperture Radar (ASAR) image using the Johns Hopkins University APL/NOAA SAR Wind Retrieval System (ANSWRS) for 0144 UTC 31 January 2008. *Image courtesy of NOAA/NESDIS/ORA/STAR and Christopher Jackson, Global Ocean Associates.* (b) The COAMPS 10-m winds from the 3-km COAMPS nested grid at 0300 UTC on the same date. Modeled wind vectors are displayed every 18 km or every sixth grid point. The SAR image, with wind vectors from the Navy Operational Global Analysis and Prediction System (NOGAPS) model, shows sharply delineated wind velocity gradients (jets) at the ends of Mindoro, Panay, and Negros islands that have close counterparts in the COAMPS model winds.

January 31, 2008, verify the presence of wind jets and wakes (see Thompson and Beal, 2000, for an explanation of how SAR measures wind stress) in the Philippines during IOP-08. Although the image is a snapshot, it agrees with the general patterns that are apparent in the mean 9-km model winds shown in Figure 1a. As in the model, the strongest winds, nearly 20 m $s^{-1}$, are in Verde Island Passage and across the southern tip of Mindoro through Tablas Strait. A suggestion of trapped mountain lee waves may be discerned at the northwest corner of Panay (11°40'N, 121°55'E) in the SAR image. Surface winds from the 3-km COAMPS at almost the same time (Figure 2b) are similar in magnitude and pattern, though the SAR winds are more coherent downwind, with sharper shear lines along the jet flanks. In particular, the wind jet emanating from the southwest corner of Panay is readily identifiable in the SAR image for more than 300 km into the Sulu Sea. Another difference is that the SAR wind maxima are stronger and more concentrated. The strongest winds in the SAR image, for example, are just to the west of Verde Island (13°35'N, 120°55'E) where the flow is constricted by the topography bordering the passage, whereas the strongest winds in the model are near Calavite Point (13°30'N, 120°15'E) where the passage opens to the South China Sea. These differences may relate to mismatches in the exact timing of atmospheric mesoscale features or may reflect the SAR product's higher resolution.

## OCEAN MODEL SURFACE CIRCULATION DURING IOP-08

Mean surface (0–50 m) currents from the 3-km resolution ocean model during IOP-08 and their associated variability (Figure 3) illustrate the primary modeled circulation characteristics of the upper ocean across the region. In the western Pacific, the North Equatorial Current is clearly evident (Figure 3a) as it divides into the poleward-flowing Kuroshio and the equatorward-flowing Mindanao currents. A mean flow of more than 1 m $s^{-1}$ enters the Philippine Archipelago through Surigao Strait (10°15'N, 125°25'E) and the Bohol Sea and flows out to the Sulu Sea through Dipolog Strait as a strong jet along the coast of Mindanao. A much weaker San Bernardino Strait (12°35'N,

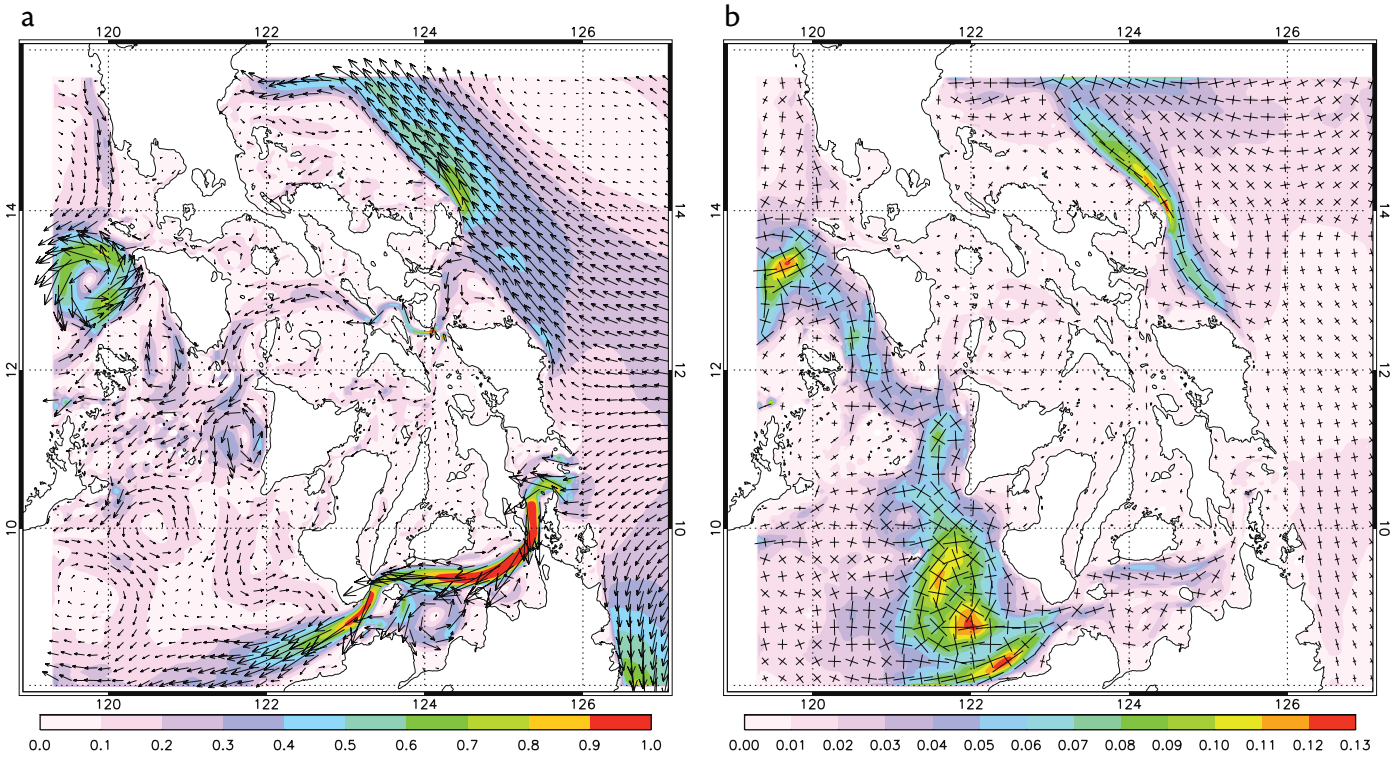


Figure 3. Navy Coastal Ocean Model (NCOM) near-surface (0–50 m) mean velocity and sea surface height from the 3-km ocean model. Sixty-day averages are from January through February 2008. (a) Surface velocity vectors with color-shaded velocity magnitude (m $s^{-1}$). (b) Surface velocity variability vectors drawn over color-shaded variability magnitude ($m^2$ $s^{-2}$).

124°10'E) flow winds through the Sibuyan Sea, enters Tablas Strait north of Tablas Island, and eventually transits to the Sulu Sea along the western edge of Cuyo East Pass (11°00'N, 121°30'E) west of Panay. Strong currents in these two straits were also observed during IOP-08 with underway acoustic Doppler current profilers (ADCP; Gordon et al., 2011) and are seen in other numerical models of the region (Han et al., 2009). A moderately strong southward flow (0.3–0.4 m $s^{-1}$) through Mindoro Strait partially recirculates along the western side of the strait. The remainder of the southerly surface flow through Mindoro Strait does not clearly connect with the flow through Tablas Strait, but flows into the Sulu Sea through the shallow Cuyo West Pass (11°20'N, 120°30'E).

Several eddies are clearly evident in the 60-day mean surface circulation pattern. The most prominent is a cyclonic eddy in the South China Sea west of Mindoro. This feature may be artificially enhanced by its proximity to the open model boundary, but it is also seen in studies with larger domains and more distant boundaries. The location and vorticity of the eddy suggests spin-up by the atmospheric wind jet emanating from Verde Island Passage (Pullen et al., 2008; Wang and Chen, 2008). Another cyclonic circulation that is visible in Cuyo East Pass between Panay and Cuyo islands was identified in the ship survey (Gordon et al., 2011) and is frequently observed in radar-derived surface currents. A third cyclonic eddy, which Gordon et al. (2011) call the Iligan Bay Eddy (11°50'N, 124°05'E), is apparent in the southwestern Bohol Sea where it was observed during all PhilEx cruises.

The greatest interisland upper-ocean velocity variability (Figure 3b) is concentrated in a band from the South China Sea through Mindoro Strait to the eastern Sulu Sea. This strip of high variability includes the junction (11°30'N, 121°40'E) of Mindoro and Tablas straits with Cuyo East Pass, an area of complex bathymetry and channeling where currents may branch or converge from three different directions. Most of this modeled nontidal variability is a consequence of strong southward flow past the islands and shallow banks in Mindoro Strait where eddies are formed and shed frequently, while some is due to occasional fluctuations of the wind that advect surface waters into and out of the connected channels. The region with the most upper-ocean current variability is found in the eastern Sulu Sea. Here, interacting currents entering and exiting the area from Cuyo East Pass and from the Bohol Sea through Dipolog Strait produce a series of energetic transitory eddies. These shallow eddies, which can be either cyclonic or anticyclonic, are confined to the deeper southern Sulu Sea basin by a submarine ridge associated with the Cagayan Island chain (9°30'N, 121°10'E). The current variability ellipses do not exhibit much directional preference in the deeper parts of the East Sulu Sea but are oriented along the bathymetry near the Cagayan Islands, Negros Island, and coastal Mindanao.

## WIND-DRIVEN UPWELLING IN VERDE ISLAND PASSAGE

The narrow Verde Island Passage (13°30'N, 121°5'E) separates Luzon and Mindoro islands and connects the South China Sea to the Sibuyan Sea. It has been identified by Carpenter and Springer (2005) as a peak region of marine biological diversity and has been designated as a priority marine conservation site by the Philippine government (Ong et al., 2002; Conservation International, 2009). In this biologically productive region, atmospheric forcing may contribute to marine ecosystem dynamics through wind-induced upwelling (Villanoy et al., 2011).

For most of IOP-08, winds blew steadily from east to west over Verde Island Passage. On several occasions during January 2008, the easterly wind briefly intensified (e.g., Pullen et al., 2011). Figure 4a shows details of the vector wind field in the passage and along the northern coast of Mindoro Island on January 31 (at the same time as the SAR image in Figure 2a), following one of the periods of increased wind. In this figure (an enlargement of the model fields from Figure 2b), winds reach a maximum of ~ 12 m $s^{-1}$ along the north coast of Mindoro and over 15 m $s^{-1}$ off the northwest shore of Mindoro. The strong, steady winds along the north coast of Mindoro are a manifestation of the Verde Island Passage topographic wind jet and favor offshore Ekman transport with subsequent nearshore upwelling of deeper water.

As an indication of an upwelling response to increased surface wind, surface waters along the north coast of Mindoro cooled noticeably on January 26 in the 1-km resolution ocean model. The cooler temperatures are evident along the coast for several days following the wind pulse. The minimum temperature, 1°C colder than ambient, was found between January 27 and January 29 in the model (Figure 4c). SST data collected during IOP-08-1 for January 30–31 clearly

show that the ship is sailing through cooler water along the northern coast of Mindoro (Figure 4d). The zonal temperature gradient in the observations is located to the east of that in the model, and observed temperatures along the ship's track are 0.5–1.0°C warmer than the model, but the basic pattern of colder temperatures is reinforced by the in situ SST. Additional evidence for upwelling in the passage during IOP-08 comes from MODIS Aqua satellite ocean color (Pacific Islands Fisheries Science Center, 2010). A composite image of chlorophyll *a* concentration for January 25–31, 2008, highlights the influence of upwelling on the phytoplankton biomass north of Mindoro (Figure 4b). Vertical temperature profiles from the model, which are in reasonable agreement with CTD measurements in the area, suggest that the upwelling is confined to the upper 60 m of the water column.

Elevated chlorophyll concentrations are frequently seen in Verde Island Passage and other Philippine

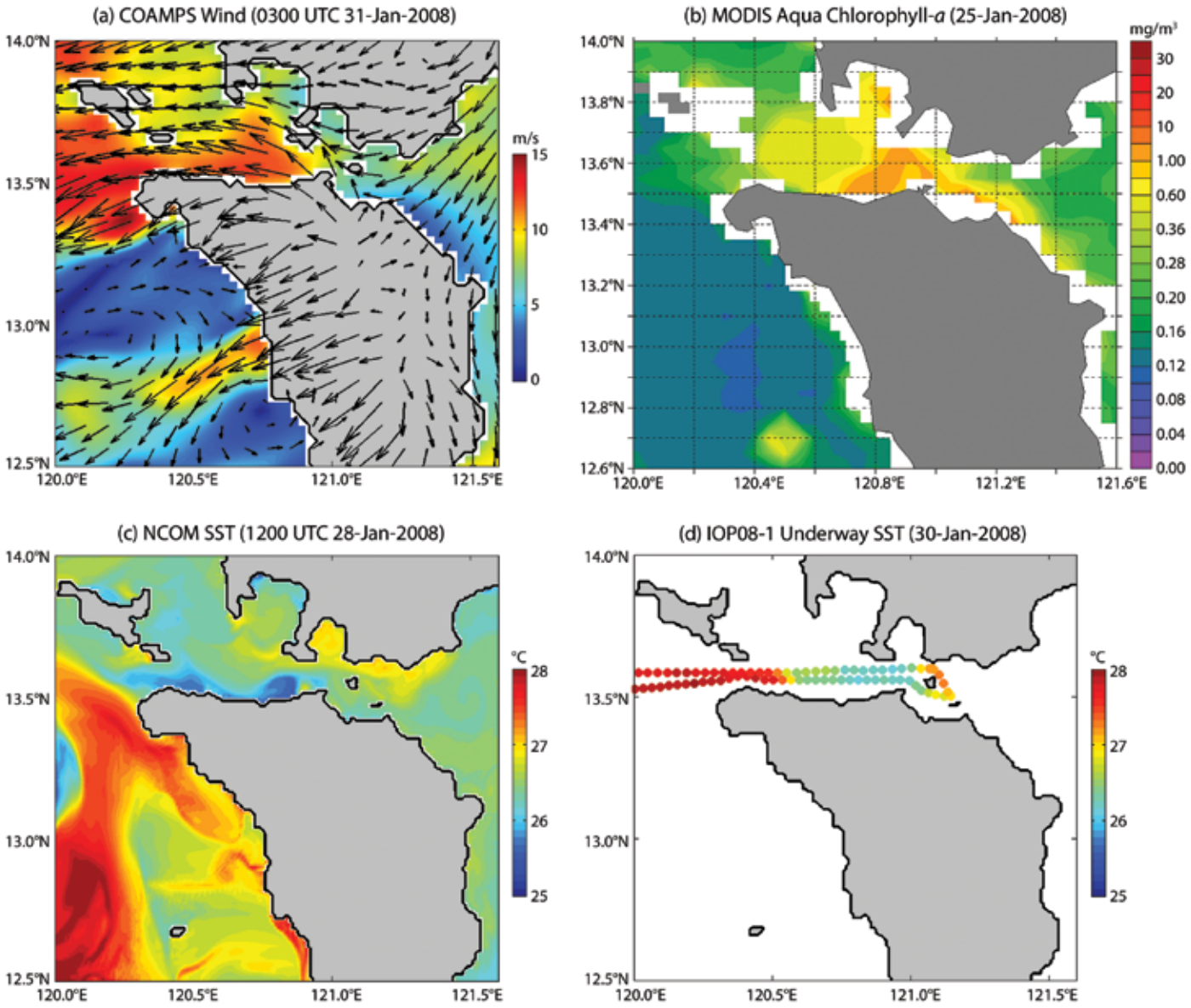


Figure 4. (a) Atmospheric model winds from 3-km nest on January 31, 2008. (b) January 25–31, 2008, MODIS Aqua composite chlorophyll *a* image (mg $m^{-3}$). (c) Ocean model sea surface temperature (SST) on 12 UTC January 28, 2008, from 1-km nest. (d) Underway shipboard SST from IOP-08-1 from January 30–31, 2008.

straits during the northeast monsoon (e.g., Figure 5a), indicating increased biological productivity and suggesting that cooler, nutrient-rich water is being transported upward into the euphotic zone by upwelling. Studies of marine life (Dolar et al., 2006; Deocadez et al., 2008) also find greater species richness and larger local populations of cetaceans and pelagic fish in these regions. A short time history of surface temperature, in the form of a Hovmöller diagram along the 120°50'E meridian (Figure 5b), shows that cooler water is present close to the northern shore of Mindoro Island during the entire month of January 2008. It also shows that the upwelling is modulated by the increasing (January 3 and 26) and decreasing (January 12) speed of the Verde Island wind jet.

## CONCLUSIONS

Coupled modeling of the atmosphere and ocean during IOP-08 and IOP-09 find that surface winds and upper-ocean currents during IOP-08 were stronger and more variable than those of IOP-09. Prominent, topographically generated wind jets in the gaps between the islands and wakes downwind of the islands are persistent features of the northeast monsoon in both 9-km and 3-km atmospheric model grids. Wind variability is greatest in the island wake regions and least in the jets. Some aspects of the coarser 3-km ocean model flow are validated by IOP-08 field study data. The "Panay Eddy," the "Iligan Bay Eddy," and strong flow through San Bernardino and Surigao straits were observed by shipboard ADCP at this time and appear in the model as prominent features.

The structure of upper-ocean current fluctuations indicates areas where the surface currents are most dynamic, including a band that extends from the west coast of Mindoro through Mindoro Strait and along Panay to Dipolog Strait. Observations support the presence of a dynamic regime along this corridor. The mean near-surface ocean flow features agree with the seasonal Regional Ocean Modeling System (ROMS) simulations that used coarser atmospheric (~ 50 km) forcing and ocean (~ 5 km) grids (Han et al., 2009). However, local details of the ocean response to wind jets and wakes and the local pattern of upwelling in Verde Island Passage are attained in the ocean model due to the finer 3-km atmospheric and 1-km ocean model grids. The presence of upwelling and nutrient-rich surface water is supported

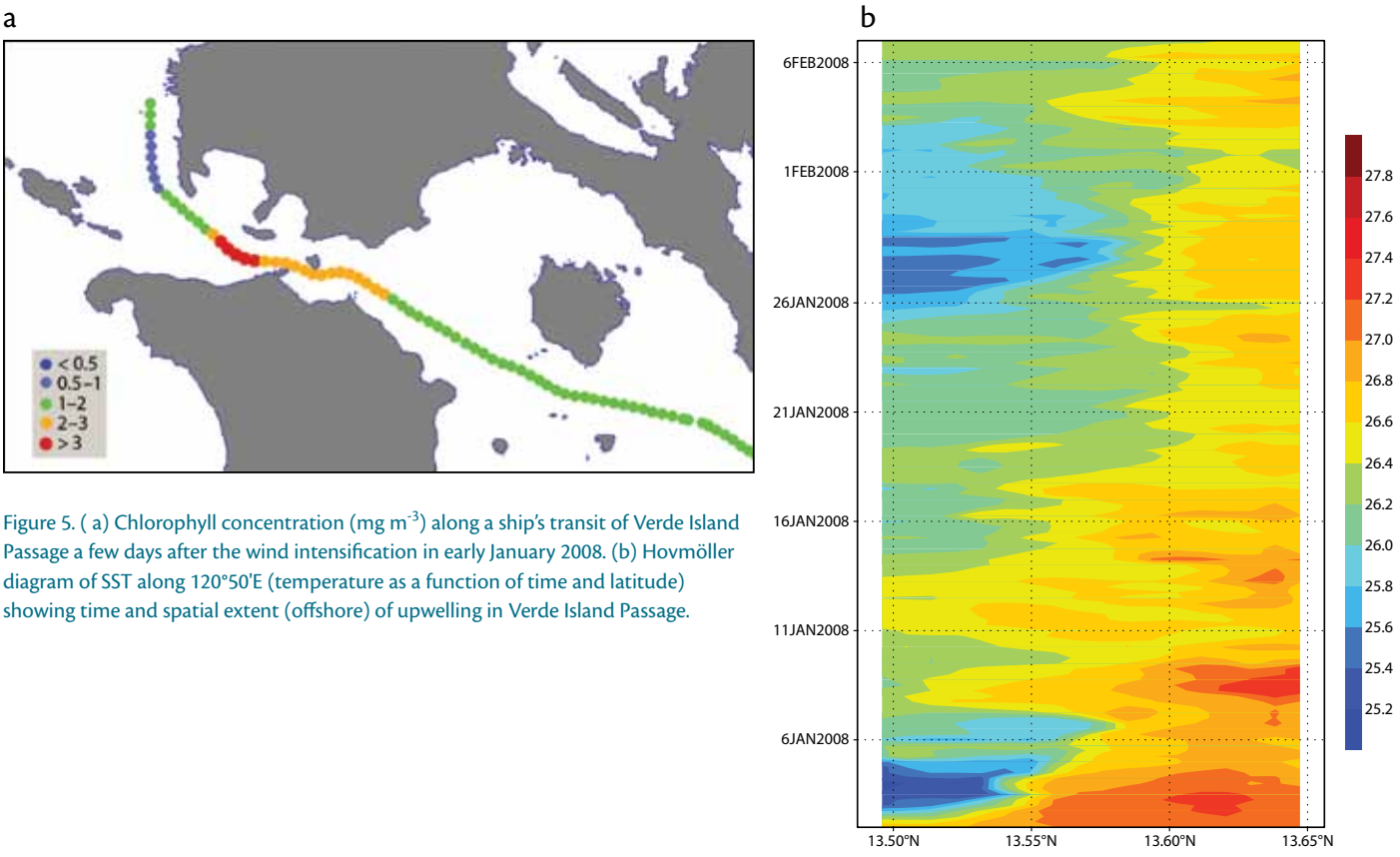


Figure 5. ( a) Chlorophyll concentration (mg $m^{-3}$) along a ship's transit of Verde Island Passage a few days after the wind intensification in early January 2008. (b) Hovmöller diagram of SST along 120°50'E (temperature as a function of time and latitude) showing time and spatial extent (offshore) of upwelling in Verde Island Passage.

by the increased chlorophyll concentrations seen in satellite imagery and in situ measurements.

## ACKNOWLEDGEMENTS

J. Doyle and P. May were supported by the Office of Naval Research (ONR) program element 0601153N. Research support for J. Pullen was provided by a Marie Tharp visiting fellowship at the Earth Institute, Columbia University; Office of Naval Research (ONR) program element 0601153N; and ONR grant N00014-10-1-0300. COAMPS is a registered trademark of the Naval Research Laboratory.

## REFERENCES

Barron, C.N., A.B. Kara, P.J. Martin, R.C. Rhodes, and L.F. Smedstad. 2006. Formulation, implementation and examination of vertical coordinate choices in the global Navy Coastal Ocean Model (NCOM). *Ocean Modelling* 11(3–4):347–375.

Burk, S.D., T. Haack, L.T. Rogers, and L.J. Wagner. 2003. Island wake dynamics and wake influence on the evaporation duct and radar propagation. *Journal of Applied Meteorology* 42:349–367.

Carpenter, K.E., and V.G. Springer. 2005. The center of the center of marine shore fish biodiversity: The Philippine Islands. *Environmental Biology of Fishes* 72:467–480.

Chang, C.-P., ed. 2004. *East Asian Monsoon*. World Scientific Series on Asia-Pacific Weather and Climate, vol. 2, 572 pp.

Chen, S., T.J. Campbell, H. Jin, S. Gaberšek, R.M. Hodur, and P.J. Martin. 2010. Effect of two-way air-sea coupling in high and low wind speed regimes. *Monthly Weather Review* 138(2):3,579–3,602.

Conservation International. 2009. *The Verde Island Passage Marine Biodiversity Conservation Corridor.* Conservation International-Philippines, Quezon City, Philippines. Available online at: http://www.conservation.org.ph/sss/Reports/verdeislandfs.pdf (accessed September 1, 2010).

Cummings, J.A. 2005. Operational multivariate ocean data assimilation. *Quarterly Journal of the Royal Meteorological Society* 131:3,583–3,604.

Deocadez, M.R., E.P. Moleño, H.O. Arceo, J.P. Cabansag, J.L. Apurado, S.S. Mamauag, C.L. Villanoy, and P.M. Aliño. 2008. Spatio-temporal patterns of juvenile and adult abundance and biomass of reef fishes in the Sulu Sea, Philippines. Pp. 999–1,003 in *Proceedings of the 11th International Coral Reef Symposium 7–11 July 2008*. International Society for Reef Studies, Ft. Lauderdale, FL.

Dolar, M.L.L., W.F. Perrin, B.L. Taylor, G.L. Kooyman, and M.N.R. Alava. 2006. Abundance and distributional ecology of cetaceans in the central Philippines. *Journal of Cetacean Research and Management* 8:93–111.

Doyle, J.D., and M.A. Shapiro. 1999. Flow response to large-scale topography: The Greenland tip jet. *Tellus* 51A:728–748.

Earth System Modeling. 2010. *ESMF*. Available online at http://www.earthsystemmodeling.org (accessed August 1, 2010).

Emery, W.J., and R.E. Thompson. 1998. *Data Analysis Methods in Physical Oceanography*. Elsevier Science, Amsterdam, 650 pp.

Fairall, C.W., E.F. Bradley, D.P. Rogers, J.B. Edson, and G.S. Young. 1996. Bulk parameterization of air-sea fluxes for TOGA COARE. *Journal of Geophysical Research* 101:3,747–3,764.

Gabersek, S.A., and D.R. Durran. 2004. The dynamics of gap flow over idealized topography. Part I: Forcing by large-scale winds in the nonrotating limit. *Journal of Atmospheric Sciences* 61:2,846–2,862.

Gordon, A.L., J. Sprintall, and A. Ffield. 2011. Regional oceanography of the Philippine Archipelago. *Oceanography* 24(1):14–27.

Han, W., A. Moore, J. Levin, B. Zhang, H. Arango, E. Curchitser, E. Di Lorenzo, A. Gordon, and J. Lin. 2009. Seasonal surface ocean circulation and dynamics in the Philippine Archipelago region during 2004–2008. *Dynamics of Atmospheres and Oceans* 47:114–137.

Hodur, R.M. 1997. The Naval Research Laboratory's Coupled Ocean/Atmosphere Mesoscale Prediction System (COAMPS). *Monthly Weather Review* 125:1,414–1,430.

Metzger, E.J., and H.E. Hurlburt. 1996. Coupled dynamics of the South China Sea, the Sulu Sea, and the Pacific Ocean. *Journal of Geophysical Research* 101:12,331–12,352.

Pacific Islands Fisheries Science Center. 2010. *OceanWatch-Central Pacific.* National Marine Fisheries Service (NOAA), Honolulu, Hawaii. Available online at http://oceanwatch.pifsc.noaa.gov.

Ong, P.S., L.E. Afuang, and R.G. Rosell-Ambal, eds. 2002. *Philippine Biodiversity Conservation Priorities: A Second Iteration of the National Biodiversity Strategy and Action Plan.* Department of Environment and Natural Resources-Protected Areas and Wildlife Bureau, Conservation International Philippines, Biodiversity Conservation Program-University of the Philippines, Center for Integrative and Development Studies, and Foundation for the Philippine Environment, Quezon City, Philippines, 113 pp.

Pullen, J., J. Doyle, P. May, C. Chavanne, P. Flament, and R. Arnone. 2008. Monsoon surges trigger oceanic eddy formation and propagation in the lee of the Philippine Islands. *Geophysical Research Letters* 35:7–10.

Pullen, J.D., A.L. Gordon, J. Sprintall, C.M. Lee, M.H. Alford, J.D. Doyle, and P.W. May. 2011. Atmospheric and oceanic processes in the vicinity of an island strait. *Oceanography* 24(1):112–121.

Qu, T. 2000. Upper-Layer Circulation in the South China Sea. *Journal of Physical Oceanography* 30:1,450–1,460.

Qu, T., Y.T. Song, T. Yamagata. 2009. An introduction to the South China Sea throughflow: Its dynamics, variability, and application for climate. *Dynamics of Atmospheres and Oceans* 47:3–14.

Shimada, T., and H. Kawamura. 2008. Double structure of the wind jet through the Tsushima Strait. *PIERS Online* 4(4):437–440, doi:10.2529/PIERS070824025140.

Smith, R.B., A.C. Gleason, P.A. Gluhosky, and V. Grubišić. 1997. The wake of St. Vincent. *Journal of Atmospheric Sciences* 54:606–623.

Smolarkiewicz, P.K., R.M. Rasmussen, and T.L. Clark, 1988. On the dynamics of Hawaiian cloud bands: Island forcing. *Journal of Atmospheric Sciences* 45:1,872–1,905.

Smolarkiewicz, P.K., and R. Rotunno. 1989. Low Froude number flow past three-dimensional obstacles. Part I: Baroclinically generated lee vortices. *Journal of Atmospheric Sciences* 46:1,154–1,164.

Thompson, D.R., and R.C. Beal. 2000. Mapping high-resolution wind fields using synthetic aperture radar. *Johns Hopkins University Technical Digest* 21:58–67.

Villanoy, C.L., O.C. Cabrera, A. Yñiguez, M. Camoying, A. de Guzman, L.T. David, and P. Flament. 2011. Monsoon-driven coastal upwelling off Zamboanga Peninsula, Philippines. *Oceanography* 24(1):156–165.

Wang, G., D. Chen, and J. Su. 2008. Winter eddy genesis in the eastern South China Sea due to orographic wind jets. *Journal of Physical Oceanography* 38:726–732.

Yoshida, S., B. Qiu, and P. Hacker. 2009. Wind generated eddy characteristics in the lee of the island of Hawaii. *Journal of Geophysical Research* 115, C03019, doi:10.1029/2009JC005417.